ELSEVIER

Physics of the Earth and Planetary Interiors 130 (2002) 235–251

PHYSICS OF THE EARTH AND PLANETARY INTERIORS

www.elsevier.com/locate/pepi

Crustal thickness, discontinuity depth, and upper mantle structure beneath southern Africa: constraints from body wave conversions

Jacek Stankiewicz [a,*], Sébastien Chevrot [b], Rob D. van der Hilst [c], Maarten J. de Wit [a]

[a] *CIGCES, Department of Geological Sciences, University of Cape Town, Rondebosch 7701, South Africa*
[b] *Observatoire Midi Pyrenees, 14 Avenue Edouard Belin, Toulouse 31400, France*
[c] *Department of Earth, Atmospheric, and Planetary Sciences, Massachusetts Institute of Technology, Cambridge, MA 02139, USA*

Received 28 June 2001; received in revised form 30 November 2001; accepted 25 February 2002

Abstract

The technique of receiver function analysis is applied to the study of crustal and upper mantle structures beneath the Kaapvaal craton in southern Africa and its surroundings. Seismic data were recorded by the seismic array of 82 sites deployed from April 1997 to April 1999 across southern Africa, as well as a dense array of 32 sites near Kimberley, in operation from December 1998 to June 1999. Arrival times for phases converted at the Moho are used to determine crustal thickness. The Moho depth in the south–western section of the craton was found to vary between 37 and 40 km, except for one station that recorded a depth of 43 km (SA23). Farther north along the western block of the craton (into Botswana) the depth increases up to 43 km. The depth increases even further in the north–eastern section of the craton, where results vary from 40 to 52 km. Just north of the Kaapvaal craton, in the neighbouring Zimbabwe craton, the crustal thickness drops significantly. The results obtained there varied from 36 to 40 km. For the Kimberley area, using the dense array, the Moho depth was found to be 37.3 km. Arrivals of the Ps and Ppps phases were used to determine the Poisson's ratio in the region. This was found to be 0.26 ± 0.01. Arrivals of phases from the 410 and 660 km mantle discontinuities are used to interpret the relative positions of these discontinuities, as well as for comparison of mantle temperatures and seismic velocities in the region with global averages. In the Kimberley area the 410 and 660 km discontinuities were found at their expected depth, implying that mantle temperatures in the region are close to the global average. The seismic velocities above the '410' were found up to 5% faster than the averages from the global *iasp91* model, which is fast even by Precambrian standards. In other sections of the Kaapvaal craton, the velocities are also faster than global averages, but not as fast as beneath Kimberley. In these sections, the '410' is also slightly elevated, while the '660' is depressed, which implies a slightly lower mantle temperature relative to the global average. Beneath the Kaapvaal craton we find evidence suggesting the presence of a zone with a reduced wavespeed gradient at an upper bound of approximately 300 km, which may mark the lower chemical boundary of the craton.

Keywords: Kaapvaal craton; Receiver functions; Seismic array

1. Introduction

Granite-greenstone assemblages of Archean age have been found on all continents and represent remnants of Earth's earliest preserved continental crust (de Wit, 1998). Worldwide, these Archean rocks

* Corresponding author. Tel.: +27-21-650-3167; fax: +27-21-650-3783.
E-mail address: jacek@cigces.uct.ac.za (J. Stankiewicz).

0031-9201/02/$ – see front matter
PII: S0031-9201(02)00012-2

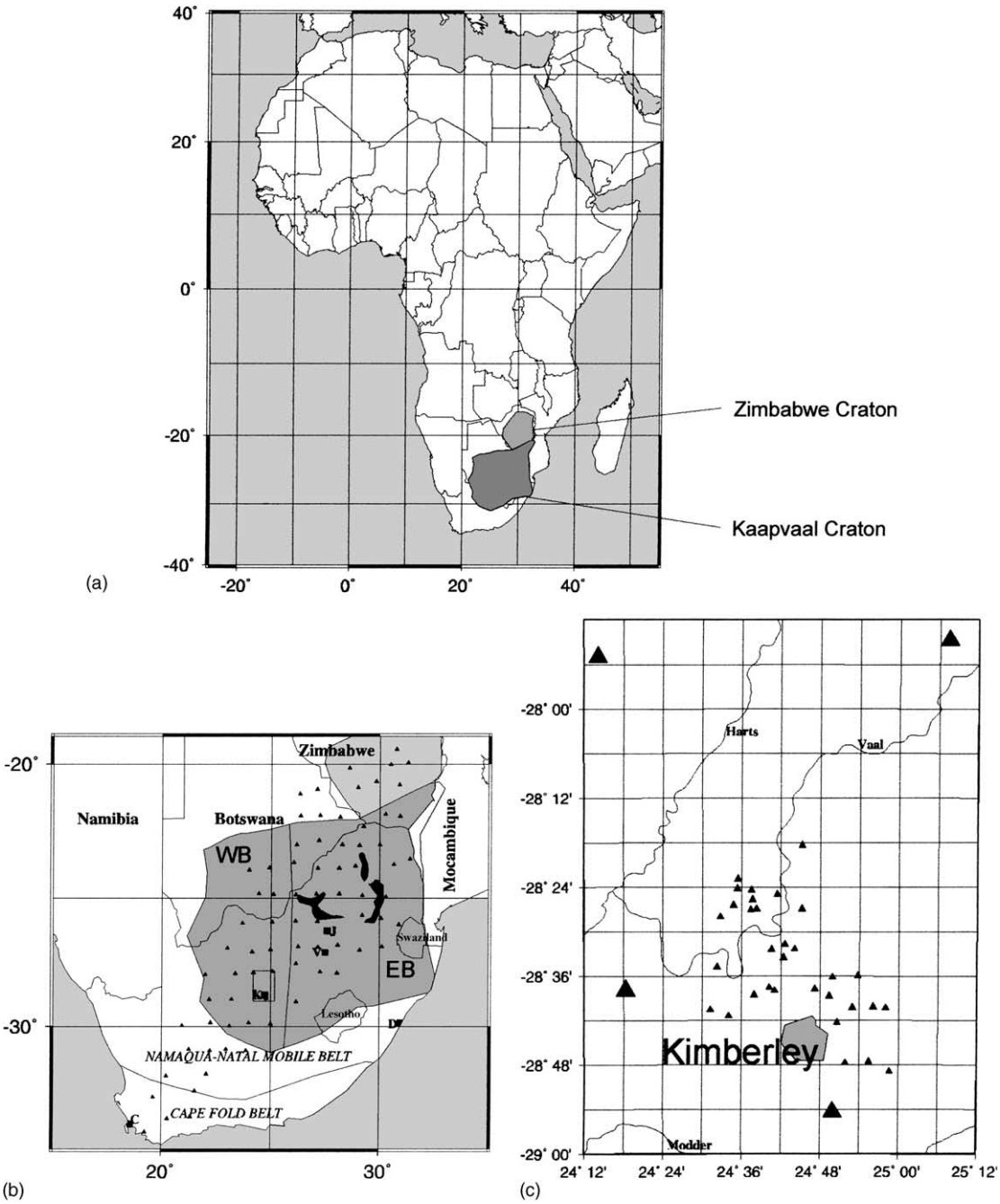

Fig. 1. (a) Locations of Kaapvaal and Zimbabwe cratons in Africa. (b) The Archean Kaapvaal craton (2.6–3.6 Ga), shaded dark gray and subdivided into eastern and western blocks (EB and WB), and the surrounding younger lithosphere, with the 82 recording sites from the regional array (filled triangles). Cape town (C), Kimberley (K), Vredefort (V), Johannesburg (J) and Durban (D) are shown for reference. Surface exposures of the bushveld complex are shown in black in northern south Africa. To the north the Zimbabwe craton is shown in pale gray. (c) The recording sites from the Kimberley array on a zoomed-in map. The four large triangles represent the regional stations adjacent to the town of Kimberley. Irregular lines represent rivers with names.

are preserved in about 10 small kernels, known as Archean cratons, embedded within the lithosphere of the present continents. Most of these cratons formed in the late Archean (2.5–3.0 Ga); those cratons with older history (early Archean, 3.0–4.0 Ga) have been deformed and metamorphosed to a large degree. The only regions that have retained substantial portions of pristine early Archean rocks are the Kaapvaal craton in southern Africa (Fig. 1a, area of 1.2×10^6 km^2) and the smaller (6×10^4 km^2) Pilbara craton in northwest Australia. The Kaapvaal craton, thus, preserves a rich geological record of the early earth (de Wit et al., 1992). It has also been suggested that the Kaapvaal craton is underlain by unusually thick (>200 km) and chemically depleted lithospheric mantle keel also largely of early Archean age (Jordan, 1975; Boyd, 1989; Pearson, 1999). This unique structure provides one of the geologic requirements for the ubiquitous diamonds that occur in the kimberlite intrusions that have subsequently penetrated the craton's upper mantle rocks (Gurney, 1990). The internal structure of this unusual upper mantle, termed the tectosphere by Jordan (1975), has yet to be revealed in detail, and a better understanding should yield new insight into the origins of Earth's early continents.

In 1996 a major interdisciplinary, multi-institutional project was started to investigate the origin and evolution of the Kaapvaal craton and its thick lithosphere (Carlson et al., 1996, 2000). The central goal of this project is to produce a tomographic image of the deep lithospheric structure of the craton using delay times of teleseismic rays. Recently, Nguuri et al. (2001) also used a receiver function analysis to study the crustal structure in southern Africa. Within the reported uncertainties the estimates on crustal thickness reported here generally concur with the results by Nguuri and co-workers. Because of the limited resolution of this technique, other studies are ongoing to complement the tomographic results.[1] For example, the precise depth to the bottom of the cratonic lithosphere cannot be deduced from tomographic studies (e.g. James et al., 2001), and further information about possible internal lithosphere structure must be deciphered using different seismological techniques (Vinnik et al., 1996). Here we attempt to analyse in greater detail the structure of the crust and the upper mantle beneath this old craton using receiver function analysis.

[1] More information on the Kaapvaal project can be found on http://kaapbase.uct.ac.za or http://www.ciw.edu/kaapvaal.

2. Method

Receiver functions are commonly used to estimate the structure of the Earth's crust and upper mantle (e.g. Langston, 1977; Chevrot and Girardin, 2000). These functions are computed from three-component seismograms and show the relative response of Earth's structure below the receiver (Ammon, 1991). The observed waveform is a composite of P-to-S converted waves that reverberate beneath the seismometer. These conversions occur when a direct wave is transmitted or reflected at an interface in Earth's interior. The simplest converted wave, Ps, occurs when the direct P-wave passes through an interface and is partially converted into an S-wave (Fig. 2). Other (usually weaker) phases consist of waveforms that pass through the interface, reflect off the Earth's surface back to the interface from which they reflect back to the recording station, converting to an S-wave during one of the reflections. Depending on the nature and the number of internal reflections the multiples are labeled, for instance, Ppps, Ppss and Psss (e.g. Ammon, 1991; Gurrola et al., 1994) and (see Fig. 2).

To observe converted Ps and other secondary phases we used a technique introduced by Vinnik (1977), which was also used in the global-scale analysis of Chevrot et al. (1999). Teleseismic seismograms are projected on the L, Q, and T axes, where L is along the principal motion direction, Q is comprised in the vertical direction and normal to L, and the transverse component, T is normal to both L and Q (Chevrot et al., 1999), and should not contain significant amounts of energy—if it does, there is a strong possibility there was a problem with the seismometer when the event was recorded. The components are then deconvolved by the principal component of the P-wave measured for a single event at all available stations. This registers all events resulting in a velocity gradient change of the P-wave, converting them into peaks or troughs, depending on whether the velocity change in positive or negative. The deconvolved *Q*-component should not have energy in the

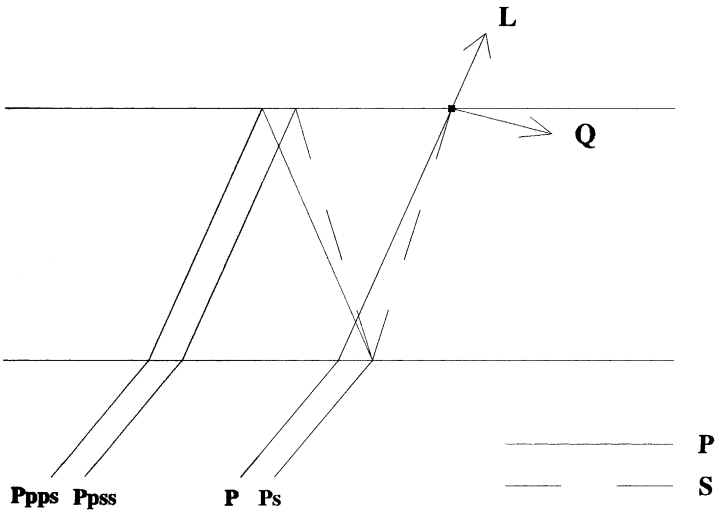

Fig. 2. Schematic ray diagram illustrating the direct P, Ps, Ppps and Ppss phases, as well as the L and Q directions.

direction of the P-wave, and the S-wave arrivals can either be reflections of the direct S-wave or Ps converted phases. This method will be used to process data from the Kimberley array.

The alternative approach (e.g. Ammon, 1991; Gurrola et al., 1994) involves deconvolving the radial component by the vertical component. The receiver functions thus obtained contain peaks at the arrival of the direct P-wave, as well as peaks and troughs marking the Ps arrivals. This approach was used to analyse the regional array data. Neither method is superior to the other one, they are both used purely for the purpose of demonstrating the alternative approaches.

Before each radial component was used for calculation, the transverse components were checked for anomalously high levels of energy, and were rejected if these were comparable with the radial component energies.

The pulses related to P-to-S conversions can be used to estimate the depth at which they were produced. For a P-wave with a vertical incidence converted to an S-wave at a depth z we have:

$$z = \Delta t \frac{v_p v_s}{v_p - v_s} \tag{1}$$

where Δt is the time between the arrival of the direct P-wave and the converted Ps phase, and v_p and v_s the respective velocities of P- and S-waves. This equation is purely hypothetical for horizontal discontinuities, as perpendicular rays do not undergo phase conversion. In reality, since the waves that reach the seismic station are not vertical (Fig. 2) a correction must be made for their angle of incidence. Eq. (1), thus, becomes (e.g. Sheriff and Geldart, 1982):

$$z = \frac{\Delta t}{[(v_s^{-2} - p^2)^{1/2} - (v_p^{-2} - p^2)^{1/2}]} = \frac{\Delta t}{q_s - q_p} \tag{2}$$

where p is the ray parameter in s/km, and q_s and q_p the vertical slownesses of the S- and P-waves, respectively.

In this model the possibility of seismic anisotropy was not taken into account, i.e. seismic waves were assumed to have the same velocity in all directions. A study by Ben-Ismail et al. (2001) revealed that Kaapvaal craton anisotropy is weak (2.64%), a result compatible with the small SKS wave splitting (0.62 s) calculated by Silver et al. (2001). These results suggest seismic anisotropy can be ignored for the purposes of this study.

3. Data

As part of the Kaapvaal craton project, portable broadband, three-component seismometers were de-

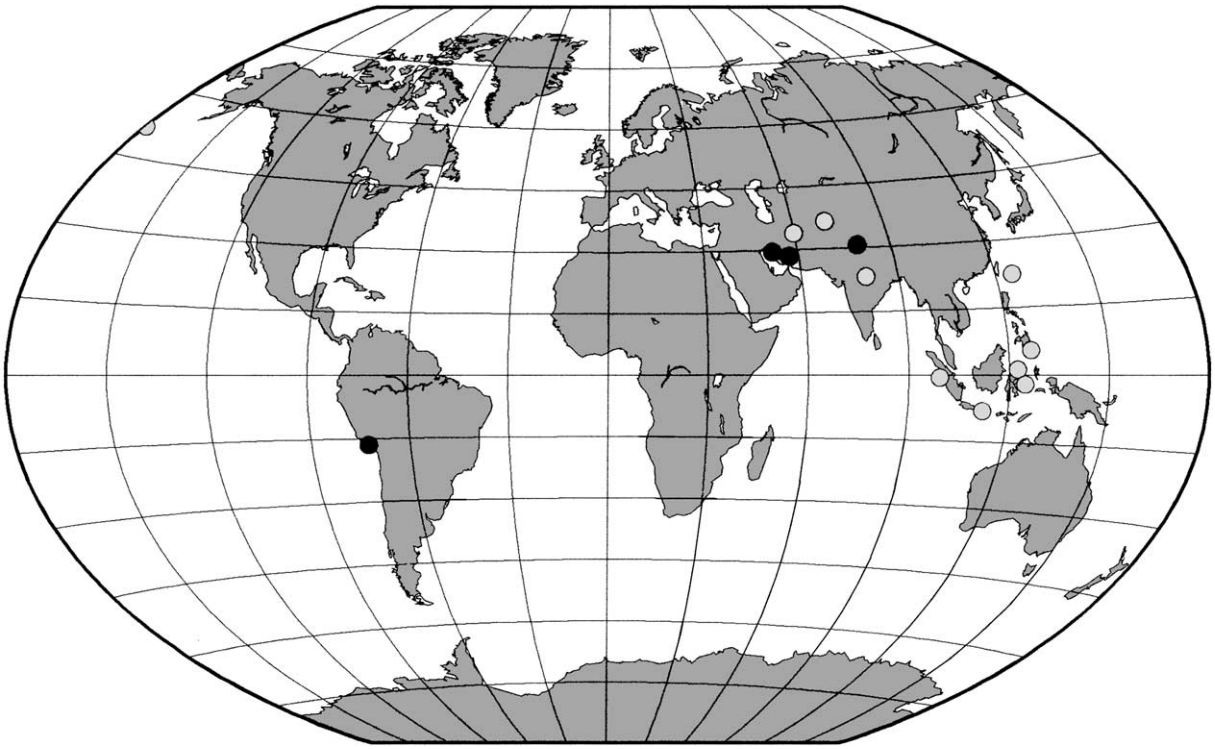

Fig. 3. Epicentres of the seismic events used in this study—shaded circles correspond to events registered by the regional array, and solid circles to the Kimberley array.

ployed in an array of 82 sites along a SW–NE axis from Cape Town to Harare (Fig. 1a). Natural teleseismic events and local mine-induced seismic activity were monitored, starting in April 1997 for a period of 2 years. In addition, a closely packed array of 32 stations was deployed near the town of Kimberley (in December 1998), which was operational for a period of 7 months (Fig. 1b).

After an analysis of the events recorded by the regional array, 10 earthquakes from different parts

Table 1
Time and locations of the seismic events registered by the regional array

Date	Latitude	Longitude	Location	Magnitude	Average back azimuth
97130	33.825N	59.809E	Iran	6.4	30.6
97133	36.411N	70.945E	Afghanistan	6.1	36.6
97141	23.083N	80.041E	India	6.0	52.2
97168	51.347N	179.332W	North Pacific	6.4	30.6
97329	1.241N	122.536E	Indonesia	6.1	92.3
98091	0.544S	99.261E	Indonesia	6.2	83.2
98123	22.306N	125.308E	Chinese sea	6.4	74.0
98245	5.410N	126.764E	Philippines	6.6	90.5
98271	8.194S	112.413E	Indonesia	6.4	96.1
98333	2.071S	124.891E	Indonesia	6.5	96.3

The dates used are in numerical format, i.e. 97130 refers to the 130th day of 1997, or the 10th May 1997. The date in that format will be used as the index for referring to individual events.

Table 2
Details of the seismic events recorded by the Kimberley array

Date	Latitude	Longitude	Location	Depth (km)	Magnitude	Average ray parameter (s/km)	Average back azimuth
99063	28.343N	57.193E	Iran	33	6.5	0.0587	31.4
99087	30.512N	79.403E	Nepal	15	6.6	0.0495	45.8
99093	16.660S	72.662W	Peru	87	6.2	0.0424	251.9
99126	29.501N	51.880E	Iran	33	6.3	0.0595	26.3

of Asia were selected (Fig. 3, Table 1). The selected records were subjected to a high-pass Butterworth filter with corner frequencies ranging between 0.2 and 0.4 Hz, depending on the amount of low frequency seismic noise. Receiver functions were then computed from the filtered traces using the programs in seismic analysis code (SAC) (Tapley and Tull, 1992).

In 7 months the Kimberley array recorded only four events of sufficient quality for our purposes (Fig. 3, Table 2). The records of different stations were stacked accounting for the varying ray parameters. Subsequently, these records were processed with a slightly different analytical method (but with the same equations) than the data from the regional array, using in this case the Seismic Handler software (Stammler, 1992), instead of SAC.

4. Results

4.1. Crustal structure and poisson's ratio

To study Moho conversions we constructed the radial components of the receiver function for each station, and we stacked them in order to reduce random noise and enhance features that are prominent throughout all individual traces. Receiver function stacks were, thus, produced for 42 stations of the regional array, with the other 40 either not functioning or recording too much seismic noise or transverse component energy to be useful for our purposes. In the successful stacks the arrival of the Ps phase converted at the Moho was identified and the time difference with the arrival of the direct P-wave determined. Assuming velocities of 6.5 and 3.8 km/s for P- and S-waves, respectively (Drummond and Collins, 1986), the depth of the Moho discontinuity was then computed using Eq. (2). The Archean Kaapvaal craton, as well as the surrounding Proterozoic mobile belts, can be divided into a number of geological terranes (de Wit et al., 1992), but with no comprehensive model for the crustal velocities variations in the terranes, the same set of velocities has been used for the entire area.

The three data samples shown in Fig. 4 yield crustal thicknesses of 40, 38 and 36 km (with an approximate uncertainty of 1 km). The calculated crustal thicknesses for all stations, as well as estimates from a previous study (Harvey et al., 2001), are shown in Fig. 5.

With one exception ($z = 43$ km), the crustal thickness in the south–western part of the craton varies between 37 and 40 km. The average depth to the Moho is 38.9 km with a standard deviation of 2.0 km. Farther north the crustal thickness decreases to 36 km, but increases again (to a value near 45 km) in southern Botswana. In the northern part of the western block the average depth is 42.1 ± 4.9 km. In the northeastern section, the crust becomes even thicker, with a number of stations recording depth over 45 km, with a maximum of 52 km. Here the average is 44.7 ± 3.4 km.

Across the northern boundary of the Kaapvaal craton, in the neighbouring Zimbabwe craton, the Moho depth decreases significantly again to between 36 and 40 km, with an average of 38.0 ± 1.6 km. Only three stations off the southern boundary of the Kaapvaal craton gave reliable results. This area, which includes the Namaqua and Cape Fold belts, has been investigated by Harvey et al. (2001). Harvey et al., (2001) found depth there to vary between 36 and 50 km, except for the southernmost station positioned right on the coast, just SE of Cape Town, for which they found a value of 28 km. The average for this area (excluding the southernmost site) was found to be 43.7 ± 2.9 km.

In another study of receiver functions, Nguuri et al. (2001) also used the regional array to estimate Moho

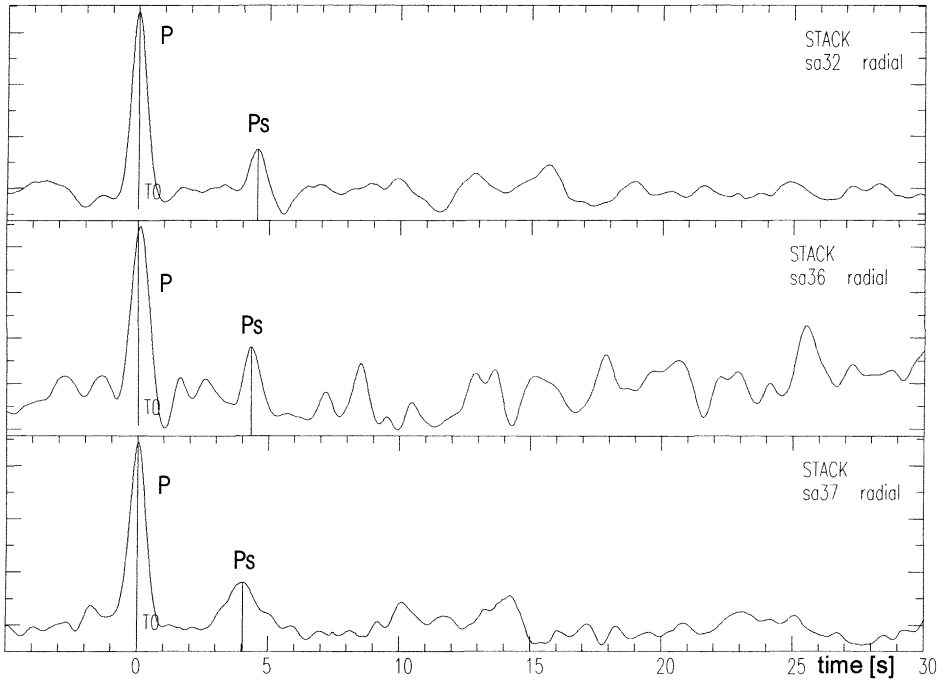

Fig. 4. Radial components of receiver functions stacked for three of the stations from the regional array. The Ps phase is clearly visible at each stack between 4 and 5 s after the P-wave.

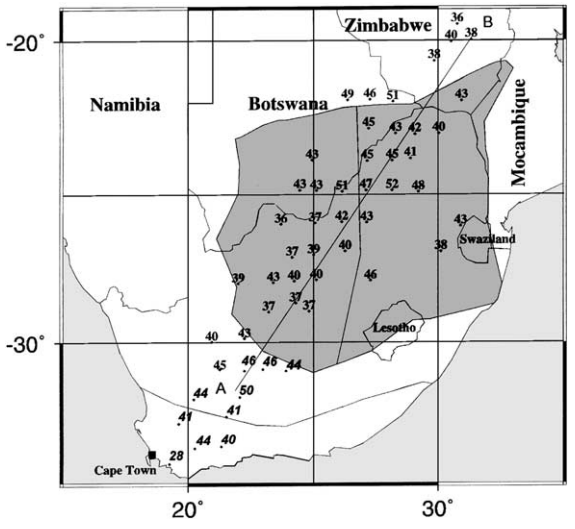

Fig. 5. Values for the crustal thickness computed from Ps phases converted at the Moho. Values in italics taken from Harvey et al. (2001). Diagonal AB is a surface projection of the cross-section in Fig. 10.

Table 3
Summary of values obtained for the crustal thickness (in km) and their comparison to results of Nguuri et al. (2001)

Area	This study	Nguuri et al. (2001)
SW Kaapvaal craton	38.9 ± 2.0	37.6 ± 2.7
NW Kaapvaal craton	42.1 ± 4.9	41.9 ± 4.3
NE Kaapvaal craton	44.6 ± 3.2	45.1 ± 2.6
Zimbabwe craton	38.0 ± 1.6	35.3 ± 0.5
South off the Kaapvaal craton	44.8 ± 3.1	45.3 ± 4.1

depth across southern Africa. Generally the results of the two studies compare very well, and the summary of the results is provided in Table 3.

For the Kimberley array, the *Q*-components of the individual receiver functions were used to produce a depth stack. This depth stack comprises a series of stacks obtained from move-out corrected records for conversions produced at successive depth. If a feature corresponds to a converted phase arrival it is expected to be best focused on the stack corresponding to the actual conversion depth. Prominent arrivals will be seen

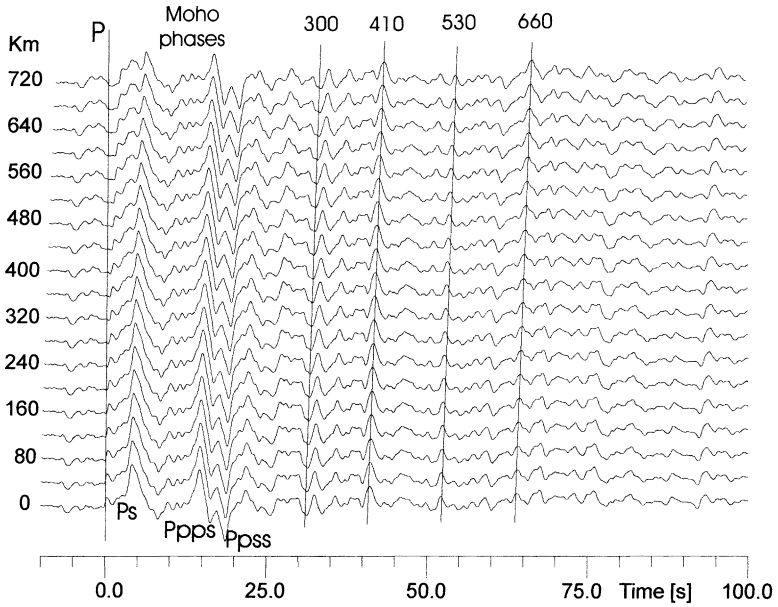

Fig. 6. P-to-S conversion depth stack for the four events recorded by the Kimberley array. P-wave arrival is at 0 s, but has no energy in the *Q*-component and, therefore, is not visible.

throughout the depth stack but will still be best defined at the individual stack corresponding to its true depth. The depth stack of P-to-S converted phases from the four selected events is shown in Fig. 6, while Fig. 7 illustrates stacks of all stations for each individual event. Steps of 40 km were used between individual stacks. The arrival of the direct P-wave is set at 0 s and is not seen on the depth stack because it has no energy in the *Q*-component. The arrival times in the depth stack could be read with an accuracy of 0.1 s.

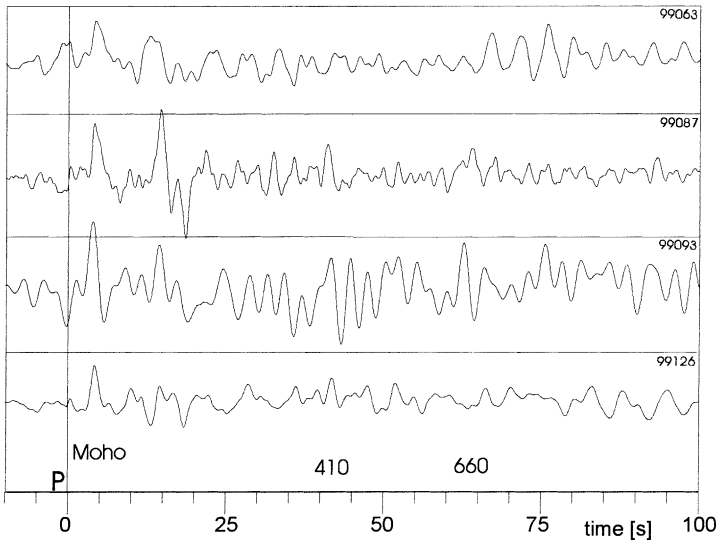

Fig. 7. *Q*-components of receiver functions of the four individual events recorded by the Kimberley array.

Taking $v_p = 6.5$ km/s and $v_s = 3.8$ km/s, as before, we obtain the crustal thickness of 37.6 ± 0.9 km from the obvious Moho conversion at 4.1 s. This is consistent with the results from the regional array (the crustal thickness near Kimberley was found to vary between 37 and 40 km). The next significant events are the Ppps arrivals and the characteristic trough of the Ppss (e.g. Ammon, 1991; Chevrot and van der Hilst, 2000). These were observed at 14.6 and 18.6 s, respectively. These phases can be used to obtain a more accurate value for the Moho depth, as well as in the calculation of the Poisson's ratio, σ, of the Kimberley crust. Poisson's ratio is a quantity related to the elasticity of a medium. It is defined as the ratio of lateral contraction to the longitudinal extension of the body when it is placed under stress (Bullen and Bolt, 1947). For an isotropic medium it can be expressed in terms of the two Lamé elastic parameters, λ and μ (the rigidity, or shear modulus):

$$\sigma = \frac{0.5\lambda}{\lambda + \mu} \tag{3}$$

A perfectly elastic solid, also known as a Poisson's medium, has $\lambda = \mu$, and in that case σ takes on a value of 0.25. A perfect fluid has $\mu = 0$, and therefore, $\sigma = 0.5$.

It is possible to express the ratio of the primary longitudinal wave velocity to that of the secondary transverse wave. The relation is (Bullen and Bolt, 1947):

$$\left(\frac{v_p}{v_s}\right)^2 = \frac{\lambda + 2\mu}{\mu} \tag{4}$$

Combining Eqs. (3) and (4) Poisson's ratio can be related to the P- and S-wave velocities via the following relation:

$$\sigma = 0.5\left[1 - \frac{1}{(v_p/v_s)^2 - 1}\right] \tag{5}$$

Simple calculation shows that when σ is 0.25, the value predicted for a perfectly elastic solid, $(v_p/v_s)^2$is equal to 3, as is often assumed for studies of the crust (Zandt et al., 1995).

The ratio provides much tighter constraints on the crustal composition than either the compressional or the shear velocity alone (Chevrot and van der Hilst, 2000). Laboratory experiments (Christensen, 1996) have shown that many physical and chemical factors may induce variations of the average crustal Poisson's ratio. The abundance of quartz ($\sigma = 0.09$) and plagioclase feldspar ($\sigma = 0.30$) have a dominant effect on the Poisson's ratio of common crustal rocks. An increase of plagioclase content and a decrease of quartz can increase the ratio from 0.24 for a granitic rock to 0.27 for a diorite, to 0.30 for a gabbro (Tarkov and Vavakin, 1982). Poisson's ratio can, therefore, be a very useful tool to trace crustal composition.

It was pointed out by Zandt et al. (1995) that it is possible to measure the crustal thickness and σ from the analysis of the travel times of the Ps and Ppps phases produced at the Moho. Defining t_1 as the time difference between arrival times of the direct P-wave and the Ps phase from the Moho, Eq. (2) can we rewritten in terms of v_p and the velocity ratio v_p/v_s:

$$t_1 = \left(\frac{h}{v_p}\right)\left[\left(\frac{v_p^2}{v_s^2} - p^2 v_p^2\right)^{1/2} - (1 - p^2 v_p^2)^{1/2}\right] \tag{6}$$

The time difference between the arrival of the Ppps phase and that of the Ps phase is simply twice the time taken by a P-wave with the given ray parameter to travel between the Moho and the surface, so if t_2 is the time between the direct P-wave arrival and that of the Ppps phase, then

$$t_2 = \left(\frac{h}{v_p}\right)\left[\left(\frac{v_p^2}{v_s^2} - p^2 v_p^2\right)^{1/2} + (1 - p^2 v_p^2)^{1/2}\right] \tag{7}$$

From Eqs. (6) and (7) it can be seen that the travel times depend on three crustal parameters: the P-wave velocity, the v_p/v_s ratio, and the crustal thickness h. The P-wave velocity for the crust was again assumed to be 6.5 km/s, the value suggested for Archean cratons by Drummond and Collins (1986).

A computer program was written to find which set of values for crustal thickness and v_p/v_s ratio yields times t_1 and t_2 that best correspond to the observed times. Of the four events used, three (99 087, 99 093 and 99 126) had prominent arrivals of the Ppps phase, and the calculation was performed for each of them. Table 4 shows the summary of results. The results are consistent, giving the average value for Poisson's ratio in the region as

$$\sigma = 0.264 \pm 0.007$$

Table 4
Results for the crustal thickness and v_p/v_s ratio analysis beneath Kimberley

Event	h (km)	v_p/v_s	σ
99087	36 ± 1	1.78 ± 0.02	0.27 ± 0.01
99093	36 ± 1	1.74 ± 0.02	0.25 ± 0.01
99126	35 ± 1	1.78 ± 0.02	0.27 ± 0.01

This is slightly higher than the 0.25 expected for a perfectly elastic solid. In the most simplified geological model of the crust, assuming it is made up entirely of quartz ($\sigma = 0.09$) and feldspar ($\sigma = 0.30$), a value of $\sigma = 0.264$ implies that feldspar makes up 83% of the crust, while quartz accounts for the other 17%. For more detailed interpretations of the ratio's implications on the crustal structure we refer to, for instance, Clarke and Silver (1993), Zandt and Ammon (1995), Christensen (1996) and Chevrot and van der Hilst (2000).

The depth of the Moho was found to vary between 35 and 36 km, consistent with earlier results in this study.

4.2. The 410, 520 and 660 km discontinuities

Techniques similar to the one used to estimate the crustal thickness in the Section 4.1 can also be used to study the structure of the upper mantle, in particular to detect and determine the depth to horizontal discontinuities. Here, we first focus on discontinuities that occur, according to the *iasp91* reference Earth model (Kennett, 1991), near 410 and 660 km depth globally. Hereinafter we will refer to these discontinuities as the "410" and "660".

The 410 km discontinuity is generally interpreted as the result of the transition from the α-phase (olivine) to the β-phase (wadsleyite) of $(Mg,Fe)_2SiO_4$ (Ito and Takahashi, 1989; Bina and Helffrich, 1994).

According to *iasp91* the Ps converted phase (referred to as $P_{410}s$) arrives 44.1 s after the P arrival. In a global study, Chevrot et al. (1999) found this time difference to vary between 41.8 and 48.7 s. This spread can be largely explained by lateral velocity variations in the upper mantle (that is, at depth < 400 km). They found that most of the observed times between 41.8 and 43.0 s are for stations located on Precambrian cratons.

For our data set, the arrivals of the $P_{410}s$ phases are not nearly as prominent as the conversions from the Moho, and owing to high noise levels only 17 regional stations could be used to identify the "410" with confidence. Fig. 8 shows examples of the constructed receiver functions. The $P_{410}s$-P differential times varied between 41.5 and 43.5 s for stations positioned on the Kaapvaal craton, while stations on the Zimbabwe craton yielded differences of about 44.5 s. Only one station south of the Kaapvaal craton gave a reliable reading (42.5 s). All these arrival times have been computed to the nearest 0.5 s. The $P_{410}s$ phase appears very prominently throughout the depth stack of the Kimberley data (Fig. 6). At the single stack corresponding to the depth of 400 km its arrival has been timed at 41.9 s.

The approach of stacking different events at individual stations (used here for the regional array data) is not ideal, because disrupted or dipping discontinuities may result in conversions at different apparent depths for different events. While the rays from different events will pass a shallow discontinuity such as the Moho a few km from each other, this error can increase to as much as 100 km for the "410", and even more for the "660"—thus, when dealing with local or tilted discontinuities this approach would not be acceptable. However, for large, prominent, uninterrupted and generally horizontal upper mantle structures that we expect here, the method can be used to obtain a first order estimate.

The nature of and depth to the 660 km has been widely discussed. Ringwood and Irifune (1988) refer to the 650 km seismic discontinuity, PREM (Dziewonski and Anderson, 1981) put the change at 670 km depth, and the *iasp91* reference Earth model has it located at 660 km depth. It has been argued that the discontinuity is caused by an isochemical phase transformation of ringwoodite (the γ phase of $(Mg,Fe)_2SiO_4$) to perovskite ($(Mg,Fe)SiO_3$) and magnesiowustite ((Mg,Fe)O) and (e.g. Anderson, 1967; Ito and Takahashi, 1989; Bina and Helffrich, 1994). Alternatively, it has been suggested that the discontinuity is associated with a change in chemical composition from an overlying upper mantle dominated by $(Mg,Fe)_2SiO_4$ olivine and spinel materials to a relatively silica-rich lower mantle composed essentially of perovskite (e.g. Ringwood and Irifune, 1988). This interpretation

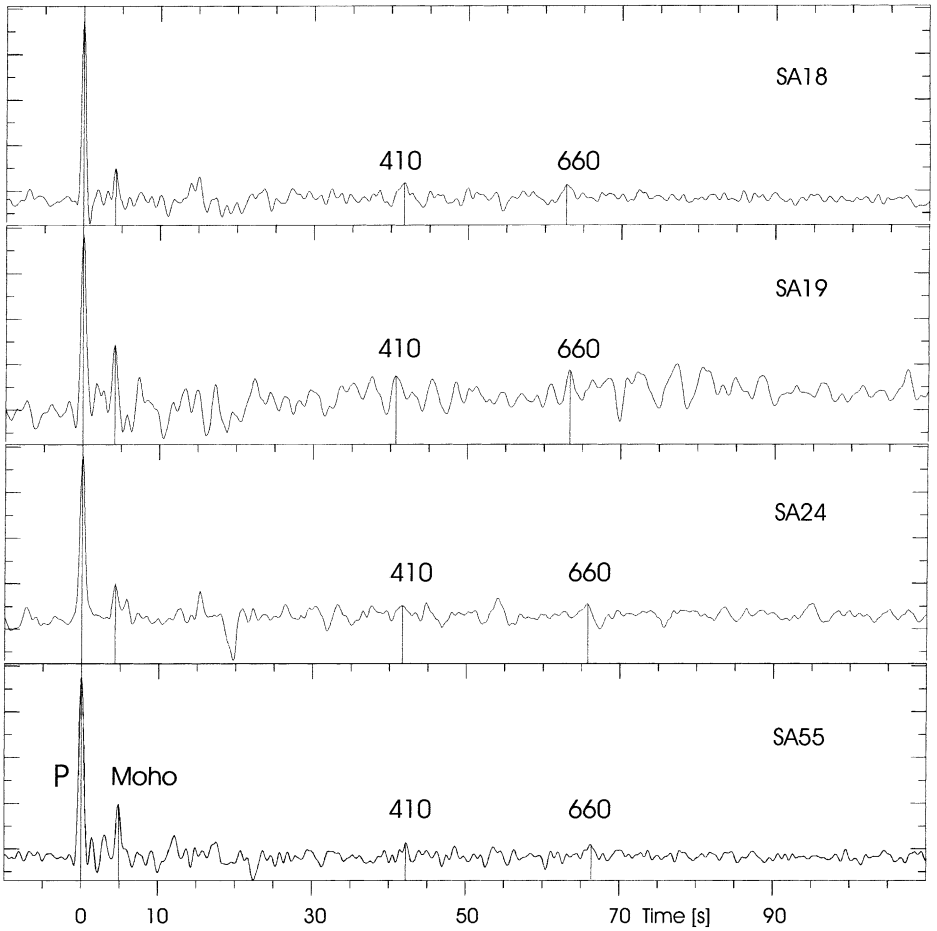

Fig. 8. Examples of radial components of the receiver functions computed from the regional array data.

would imply that the 660 km discontinuity separates convective systems in the upper and lower mantle. In the case of a chemical boundary the topography of the "660" would depend on the density contrast whereas for the iso-chemical phase transformation it is controlled by the Clapeyron slope, that is, the temperature dependence of the pressure at which the transition occurs. The magnitude of the topography puts important constraints on the style of mantle convection (e.g. Ringwood and Irifune, 1988; Machetel and Weber, 1991; Tackley et al., 1993; Schubert and Tackley, 1995).

In their global study of Ps phases, Chevrot et al. (1999) found that most $P_{660}s$ move-out corrected (with a reference slowness of 6.4 s/degree) phases arrive between 65.6 and 72.7 s after the direct P-wave. The *iasp91* model predicts it at 68.0 s. The arrivals in this study were even less clear then those of $P_{410}s$, with only 15 of the stations registering convincing peaks near the expected time. Most of the selected regional array traces yielded times within 1 s from the global average of 68 s, the exceptions being three stations near Kimberley, which registered arrivals <66 s after the direct P-wave. In the Kimberley data depth stack the $P_{660}s$ is not very clear in the shallower stacks, but focuses clearly as a peak at 65.7 s at the correct depth.

The existence of a discontinuity at $\sim$520 km has been reported by a few authors (e.g. Revenaugh and Jordan, 1991; Dueker and Sheehan, 1998; Deuss and Woodhouse, 2001), and no definitive physical or

chemical explanation for its existence has been suggested. In the depth stacks determined here a small peak appears fairly consistently near 53.3 s, which corresponds to a depth of about 530 km. It suggests the presence of a discontinuity, but does not provide conclusive evidence for it, as we cannot rule out that the peak could be a reverberation of an earlier phase.

4.3. Transition zone thickness and wavespeed

Experimental mineral physics suggests that the Clapeyron slopes of the phase transformations at 410 and 660 km depth are inversely correlated—lower (higher) than average temperatures will elevate (depress) the "410" while the opposite is expected for the "660" (e.g. Ito and Takahashi, 1989; Bina and Helffrich, 1994). The thickness of the transition zone between these discontinuities will thus depend on mantle temperature—in relatively hot regions the thickness of the transition zone is expected to be thinner than in cooler ones. Accurate measurements of the depth to the discontinuities would enable one to determine whether the transition zone is relatively "hot" or "cold". To determine the depth one needs the time difference between arrivals of $P_{410}s$ and $P_{660}s$ phases as well as information about the wave speeds in the transition zone and above (Lebedev et al., 2002). Once the depth to the "410" is determined the $P_{410}s$ travel time can be used to constrain the propagation speed of the seismic waves in the upper mantle (i.e. above 410 km depth).

In *iasp91* the time difference between arrivals of $P_{410}s$ and $P_{660}s$ is 23.9 s. Most stations on the Kaapvaal craton yield time differences between 25.0 and 26.5 s, that is, larger than the global average. In contrast, stations near the town of Kimberley yielded differences between 23.5 and 24.0 s, which is consistent with the global average. For stations on the Zimbabwe craton the time difference was around 23.5 s, while the single station over the southern boundary of the Kaapvaal craton gave a reading of just under 24 s.

In as far as they reflect variations in the thickness of the transition zone beneath the stations, these differential times imply that for most of the Kaapvaal craton this zone is wider than the global average of 250 km. In turn, this suggests that its temperature is lower than average. If the difference in transition zone thickness is split equally between the two discontinuities then the "410" is elevated possibly by >10 km, while the "660" is lowered by the same amount. Beneath Kimberley the transition zone thickness is inferred to be close (that is, within 2%) to the global average depth of 250 km, which would suggest that the two discontinuities are near their expected depth and the mantle temperature close to the global average (but warmer than the surrounding mantle). For the Zimbabwe craton the data suggest that the transition zone is thinner than average, with the discontinuities shifted towards each other by about 5 km. Results from the station to the south of the Kaapvaal craton imply an average mantle temperature, and no significant shift in position of the two discontinuities is required. A summary of these results is given in Table 5.

If we assume the approximate positions of the "410 km" discontinuity, and this solution is clearly non-unique, the arrival times of the $P_{410}s$ phases can be used to estimate seismic velocities in the upper mantle (depth $<$ 400 km) relative to the global average velocities in the *iasp91* model. Near Kimberley the "410" is assumed to be very close to its namesake depth, but at the stations in that area the $P_{410}s$ phase arrived >2 s earlier than the predicted value of 44.1 s (Kennett and Engdahl, 1991). This would suggest that beneath Kimberley uppermost mantle

Table 5
Summary of results for the upper mantle properties

	Kimberley area	NW Kaapvaal craton	NE Kaapvaal craton	SW mobile belts	Zimbabwe craton	*Iasp91* averages
Moho depth (km)	35.3	38.8	40.9	44.1	34.8	35.0
Transition zone thickness (km)	250	270	270	250	240	250
"410" depth (km)	410	400	400	410	415	410
"660" depth (km)	660	670	670	660	655	660
v/v_{iasp91} above 400 km	1.05	1.02	1.02	1.01	1.00	1.00
Low velocity zone	Yes	Yes	Yes	No	No	No

velocities beneath Kimberley are up to 5% faster than the global average. In other regions of the Kaapvaal craton $P_{410}s$ arrivals were similar to those recorded by sites near Kimberley, but the $P_{660}s$ arrivals suggested the "410" to be elevated by 10 km or more. Although they are faster than the global average by up to 2%, the velocities in these regions may thus not be as high as beneath Kimberley. Stations on the Zimbabwe craton registered the arrivals from the slightly (probably <5 km) depressed "410" slightly (<0.5 s) later than the global average of 44.1 s. This suggests that mantle velocities are very close to the averages from the *iasp91* model. One would hesitate to treat a single station off the southern edge of the craton as a reliable source of information, but a slightly early arrival time from a discontinuity that is not displaced would imply seismic velocities faster by up to 1% than the global average.

The Kimberley array results give a travel time of the converted S-wave through the transition zone as 23.8 s. Vinnik et al. (1996) observed the two phase arrivals at 41.8 and 65.6 s, respectively, also implying a travel time of 23.8 s. The inferred time difference is also very close to the 23.9 s predicted by the *iasp91* model (Kennett and Engdahl, 1991) and repeated in the global study of Chevrot et al. (1999). This suggests that the 410 and 660 km discontinuities beneath Kimberley occur very close to their namesake depth, i.e. 410 and 660 km, respectively. It can, therefore, also be concluded that the data are consistent with an upper mantle temperature in this region that is similar to the global average. These results are consistent with the ones obtained from the regional array for the Kimberley area.

The individual arrival times of the converted phases concerned are significantly earlier than the values of 44.1 and 68.0 s from the *iasp91* model. This is again consistent with the results from Section 4.3, and suggests that the upper mantle velocities beneath Kimberley are up to 5% faster than the global average, which is fast even by Precambrian standards, in fact these values are higher than anywhere else analysed by Chevrot et al. (1999).

4.4. Existence of a sub-continental low velocity zone

Many Archean cratons are associated with a low velocity zone starting at a depth of about 300 km (e.g.

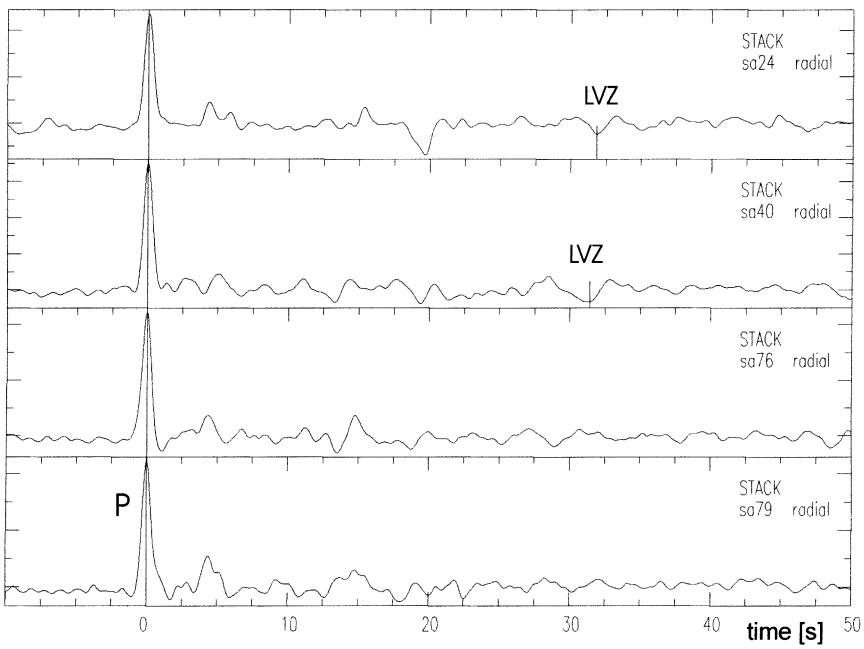

Fig. 9. Radial components of two stations on the Kaapvaal craton (sa24 and sa40) and two on the Zimbabwe craton (sa76 and sa79). The trough suggesting a low velocity zone is visible at $t \approx 32$ s. only for the Kaapvaal stations.

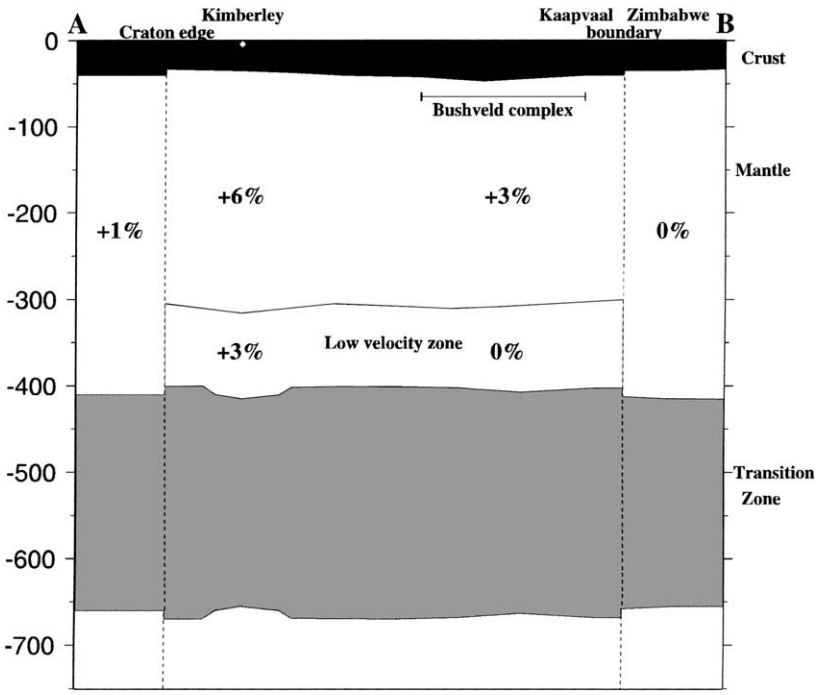

Fig. 10. Cross-section of the crust and upper mantle showing all the features discussed in the text. Percentages indicate how seismic velocities in a given zone differ from the global average for that depth.

LeFevre and Helmberger, 1989; Vinnik et al., 1996). If the upper boundary of such a zone has a sufficiently steep gradient, or is discontinuity, it will produce a P-to-S converted wave which would register a trough in the receiver function. The existence of the low velocity zone has been suggested but the depth has remained enigmatic. From surface wave studies Qui et al. (1996) and Priestley (1999) suggested its upper bound to be shallower than 200 km, while Vinnik et al. (1996) use converted phases to claim that the zone does not extend further than 50 km above the 410 km discontinuity.

In the depth stack of the Kimberley data (Fig. 6) two phases are observed at 31.9 and 34.2, corresponding to focusing stack depth of about 305 and 330 km, respectively. The troughs seem sufficiently prominent to suggest that the reduced wavespeed gradient zone does in fact exist beneath the Kaapvaal craton. Our observations suggest, however, that the upper boundary of the zone occurs at depth different to those suggested by Vinnik et al. (1996), Qui et al. (1996) and Priestley (1999). Our result is consistent with results from Freybourger et al. (2001), who showed there is no evidence for such a zone at depth less than 250 km. The presence of two troughs instead of just one could mean that the low velocity zone is a fairly complex feature, with the velocities decreasing at 305 km, and then decreasing even further at 330 km. This zone may mark the lower chemical boundary of the Kaapvaal craton.

Similar results were observed in the data from the regional array, but they were not as robust and more research is necessary to make them conclusive. A low velocity zone was only detected beneath the Kaapvaal craton stations, further illustrating the difference between the Kaapvaal and Zimbabwe cratons (Fig. 9).

Fig. 10 summarises the results for the upper mantle properties obtained in the study.

5. Discussion and conclusions

In the first part of this study we showed how receiver functions can be used to study discontinuities in the

lithosphere by analyzing variations of the crustal thickness and depth to deeper discontinuities beneath the surface of the Kaapvaal craton and its surroundings. Off the craton's south–western boundary values for the crustal thickness vary around 45 km and decrease to between 37 and 40 km toward the southern section of the craton. Farther north the Moho depth increases to 52 km. These larger crustal thicknesses coincide with the surface exposure of the 2.06 Ga Bushveld complex, the world's largest mafic layered intrusion, and it is likely that the thick crust here includes Paleoproterozoic addition to the Archean crust in this region (Nguuri et al., 2001; Doucouré and de Wit, in press). North of the Kaapvaal craton (on the Zimbabwe craton) stations record depth between 33.0 and 36.0 km.

Our analysis of converted phases suggests that for most of the Kaapvaal craton the mantle transition zone, between the 410 and 660 km discontinuities, has a greater than global average thickness, possibly by >20 km. If we assume that the 410 km discontinuity is shifted upwards by about half that distance (∼10 km), the earlier than expected arrival times of the P_{410}s phases imply the seismic velocities in the upper mantle beneath the craton are above the global average. This is consistent with earlier findings (e.g. Vinnik et al., 1995, 1996).

In the Kimberley region, however, our observations are consistent with the transition zone having exactly the expected thickness, and the two discontinuities can thus be expected to occur close to their namesake depth. The early arrival times of the P_{410}s are representative of large parts of the Kaapvaal craton, confirming the results of Chevrot et al. (1999) that the seismic velocities in this region are fast even by Archean cratonic mantle standards.

By relating the thickness of the transition zone to the relative upper mantle temperature, our results suggest that while the temperatures beneath the Kimberley area are close to global averages, the surrounding upper mantle is considerably cooler. The results for the neighbouring Zimbabwe craton suggest a slightly thinner than average transition zone, and thus, somewhat higher temperatures than below the Kaapvaal craton. Here the seismic velocities are close to the global averages from the *iasp91* model, and therefore, relatively slow for an Archean craton. Our data, therefore, suggest that the deep structure of the two neighbouring cratons differ from each other.

A cool mantle is not necessarily inconsistent with the high heat flow across southern Africa as reported, for instance, by Nyblade et al. (1990) and Nyblade and Pollack (1993), which has been associated with southern Africa's abnormal elevation known as the African Superswell (e.g. Nyblade and Robinson, 1994; Lithgow-Bertelloni and Silver, 1998). From studies of heat flow in the Witwatersrand Basin and the Vredefort structure, Hart (1978), Nicolaysen et al. (1981), Welke and Nicolaysen (1981), Jones and Bottomley (1986) and Jones (1988) found that excessive heat production is generated in the crust. Our results confirm that the lithospheric mantle of the Kaapvaal craton is actually relatively cold, and therefore, cannot be responsible for an abnormally high heat flow, nor for the topographic swell related to it.

Finally, we also found evidence suggesting the presence of a low velocity zone with an upper bound of approximately 300 km beneath the Kaapvaal craton. We believe this zone reflects the complex base of the craton.

Acknowledgements

The authors would like to thank Moctar Doucouré, Rod Green, David James, Steve Gao and the rest of the Kaapvaal Seismic Group. The study was funded by the National Research Foundation in South Africa, with additional financial support from Carnegie Institution of Washington and the Massachusetts Institute of Technology. The Figs. 1–3, 5 and 10 were done using generic mapping tools ((GMT)—Wessel and Smith, 1991). We thank two anonymous reviewers for their scrutiny and helpful suggestions towards improving this paper.

References

Ammon, C.J., 1991. The isolation of receiver effects from teleseismic P-waveforms. Bull. Seism. Soc. Am. 81, 2504–2510.

Anderson, D.L., 1967. Latest information from seismic observations. In: T.F. Gaskell (Ed.), The Earth's Mantle. Academic Press, New York, pp. 355–420.

Ben-Ismail, W., Barruol, G., Mainprice, D., 2001. The Kaapvaal craton seismic anisotropy: petrophysical analyses of upper mantle kimberlite nodules. Geophys. Res. Lett. 28, 2497–2500.

Bina, C., Helffrich, G.R., 1994. Phase transition Clapeyron slopes and transition zone seismic discontinuity topography. J. Geophys Res. 99, 15853–15860.

Boyd, F.R., 1989. Compositional distinction between oceanic and cratonic lithosphere. Earth Planet. Sci. Lett. 96, 15–26.

Bullen, K.E., Bolt, B.A., 1947. An Introduction to the Theory of Seismology. Cambridge University Press, Cambridge.

Carlson, R.W., Grove, T.L., de Wit, M.J., Gurney, J.J., 1996. Program to study crust and mantle of the Archean craton in southern Africa. Eos. Am. Geophys. Union 77, 273–277.

Carlson, R.W., Boyd, F.R., Shirey, S.B., Janney, P.E., Grove, T.L., Bowring, S.A., Schmitz, M.D., Dann, J.C., Bell, D.R., Gurney, J.J., Richardson, S.H., Tredoux, M., Menzies, A.H., Pearson, D.G., Hart, R.J., Wilson, A.H., Moser, D., 2000. Continental growth, preservation and modification in southern Africa. GSA Today 10, 1–7.

Chevrot, S., Girardin, N., 2000. On the detection and identification of converted and reflected phases from receiver functions. Geophys. J. Int. 141, 801–808.

Chevrot, S., van der Hilst, R.D., 2000. The Poisson's ratio of the Australian crust: Geological and geophysical implications, submitted to EPSL.

Chevrot, S., Vinnik, L.P., Montagner, J.P., 1999. Global-scale analysis of the mantle Pds phases. J. Geophys. Res. 104, 20203–20219.

Christensen, N.I., 1996. Poisson's ratio and crustal seismology. J. Geophys. Res. 101, 3139–3156.

Clarke, T.J., Silver, P.G., 1993. Estimation of crustal Poisson's ratio from broad band teleseismic data. Geophys. Res. Lett. 20, 241–244.

Deuss, A., Woodhouse, J., 2001. Seismic observations of splitting of the mid-transition zone discontinuity in Earth's mantle. Science 294, 354–357.

de Wit, M.J., 1998. On Archean granites, greenstones, cratons and tectonics: does the evidence demand a verdict? Precambrian Res. 91, 181–226.

de Wit, M.J., Roering, C., Hart, R.J., Armstrong, R.A., de Ronde, C.E.J., Green, R.W.E., Tredoux, M., Peberdy, E., Hart, R.A., 1992. Formation of an Archean continent. Nature 357, 553–562.

Doucouré, C.M., de Wit, M.J., in press. Temporary variations in rigidity and mechanical behaviour of old thick continental lithosphere, S. Afr. J. Geol.

Drummond, B.J., Collins, C.D.N., 1986. The nature of the crust–mantle boundary under Australia from seismic evidence. In: The Australian Lithosphere, Geol. Soc. Aust. Spec. Publ., pp. 67–80.

Dueker, K.G., Sheehan, A.F., 1998. Mantle discontinuity structure beneath the Colorado Rocky mountains and high plains. J. Geophys. Res. 103, 7153–7169.

Dziewonski, A.M., Anderson, D.L., 1981. Preliminary reference earth model. Phys. Earth. Planet. Inter. 25, 297–356.

Freybourger, M., Gaherty, J.B., Jordan, T.H. and the Kaapvaal Seismic Group, 2001. Structure of the Kaapvaal craton from surface waves. Geophys. Res. Lett., 28, 2489–2492.

Gurney, J.J., 1990. The diamondiferous roots of our wandering continents. Trans. Geol. Soc. S. Afr. 93, 424–437.

Gurrola, H., Minster, J.B., Owens, T.J., 1994. The use of velocity spectrum for stacking receiver functions and imaging upper mantle discontinuities. Geophys. J. Int. 117, 427–440.

Hart, R.J., 1978. A study of the isotopic and geochemical gradients in the Old Granite of the Vredefort Structure, with implications to continental heat flow. PhD Thesis, University of Witwatersrand.

Harvey, J.D., de Wit, M.J., Stankiewicz, J., Doucouré, C.M., 2001. Structural variations of the crust in the south–western Cape, deduced from seismic receiver functions. S. Afr. J. Geol. 104, 231–242.

Ito, E., Takahashi, E., 1989. Postspinel transformations in the system Mg_2SiO_4-Fe_2SiO_4 and some geophysical implications. J. Geophys. Res. 94, 10637–10646.

James, D.E., Fouch, M.J., VanDecar, J.C., van der Lee, S. and the Kaapvaal Seismic Group 2001. Tectospheric structure beneath south Africa, Geophys. Res. Lett., 28, 2485–2488.

Jones, M.Q.W., 1988. Heat flow in the Witwatersrand basin and environs and its significance for the south African shield geotherm and lithosphere thickness. J. Geophys. Res. 93, 3243–3260.

Jones, M.Q.W., Bottomley, P., 1986. Geothermal gradients and heat flow in the Witwatersrand basin. Presented at Geocongress'86: The 21st Biennial Congress, Geol. Soc. of S. Afr., University of Witwatersrand, Johannesburg.

Jordan, T.H., 1975. The continental tectosphere. Rev. Geophys 13, 1–12.

Kennett, B., 1991. Seismic velocity gradients in the upper mantle. Geophys. Res. Lett. 18, 115–118.

Kennett, B., Engdahl, E.R., 1991. Travel times for global earthquake location and phase identification. Geophys. J. Int. 105, 429–465.

Langston, C.A., 1977. The effects of planar dipping structure on source and receiver responses for constant ray parameter. Bull. Seism. Soc. Am. 67, 1029–1050.

Lebedev, S., Chevrot, S., van der Hilst, R.D., 2002. Seismic evidence for olivine phase changes at the 410- and 660-kilometer discontinuities. Science, Vol. 296, in press.

LeFevre, L.V., Helmberger, D.V., 1989. Upper mantle P velocity structure of the Canadian Shield. J. Geophys. Res. 94, 17749–17765.

Lithgow-Bertelloni, C., Silver, P.G., 1998. Dynamic topography, plate driving forces, and the African superswell. Nature 395, 269–273.

Machetel, P., Weber, P., 1991. Intermittent layered convection in a model mantle with an endothermic phase change at 670 km. Nature 350, 55–57.

Nguuri, T.K., Gore, J., James, D.E., Webb, S.J., Wright, C., Zengeni, T.G., Gwavava, O., Snoke, J.A., 2001. Crustal structure beneath southern Africa and its implications for the formation and evolution of the Kaapvaal and Zimbabwe cratons. Geophys. Res. Lett. 28, 2501–2504.

Nicolaysen, L.O., Hart, R.J., Gale, N.H., 1981. The Vredefort radioelement profile extended to supercrustal strata at Carletonville, with implications for continental heat flow. J. Geophys. Res. 86, 10653–10661.

Nyblade, A.A., Pollack, H.N., Jones, D.C., Podmore, F., Mushayandebvu, M., 1990. Terrestrial heat flow in east and southern Africa. J. Geophys. Res. 95, 17371–17384.

Nyblade, A.A., Pollack, H.N., 1993. A global analysis of heat flow from Precambrian terrains: Implications for the thermal structure of Proterozoic and Archean lithosphere. J. Geophys. Res. 98, 12207–12218.

Nyblade, A.A., Robinson, S.W., 1994. The African Superswell. Geophys. Res. Lett. 21, 765–768.

Pearson, D.G., 1999. The age of continental roots. Lithos 48, 171–194.

Priestley, K., 1999. Velocity structure of the continental upper mantle: evidence from southern Africa. Lithos 48, 45–46.

Qui, X., Priestley, K., McKenzie, D., 1996. Average lithospheric structure of southern Africa. Geophys. J. Int. 127, 563–587.

Revenaugh, J., Jordan, T.H., 1991. Mantle layering from ScS reverberations: 2. The transition zone. J. Geophys. Sci. 96, 19763–19780.

Ringwood, A.E., Irifune, T., 1988. Nature of the 650 km seismic discontinuity: implications for mantle dynamics and differentiation. Nature 331, 131–136.

Schubert, G., Tackley, P.J., 1995. Mantle dynamics: The strong control of the spinel–perovskite transition at a depth of 660 km. J. Geodynamics 20, 417–428.

Sheriff, R.E., Geldart, L.P., 1982. Exploration Seismology. Cambridge University Press, New York, Vol. 1, pp. 82–101.

Silver, P.G., Gao, S.S., Liu, K.H., and the Kaapvaal Seismic Group, 2001. Mantle deformation beneath southern Africa. Geophys. Res. Lett., 28, 2493–2496.

Stammler, K., 1992. Seismic Handler, User's Manual, attachment to PhD thesis at the Seismological Central Observatory, University of Erlangen.

Tapley, W.C., Tull, J.E., 1992. SAC—Seismic Analysis Code USER'S MANUAL. Regents of the University of California, CA.

Tackley, P.J., Stevenson, D.J., Glatzmaier, G.A., Schubert, G., 1993. Effects of an endothermic phase transition at 670 km depth in a spherical model of convection in the Earth's mantle. Nature 361, 699–704.

Tarkov, A.P., Vavakin, V.V., 1982. Poisson's ratio behaviour in crystalline rocks: application to the study of the Earth's interior. Phys. Earth Planet. Inter. 29, 24–29.

Vinnik, L.P., 1977. Detection of waves converted from P to SV in the mantle. Phys. Earth planet. Inter. 15, 39–45.

Vinnik, L.P., Green, R.W.E., Nicolaysen, L.O., 1995. Recent deformation of the deep continental root beneath southern Africa. Nature 375, 50–52.

Vinnik, L.P., Green, R.W.E., Nicolaysen, L.O., Kosarev, G.L., Petersen, N.V., 1996. Deep seismic structure of the Kaapvaal craton. Tectonophysics 262, 67–75.

Welke, H., Nicolaysen, L.O., 1981. A new interpretive procedure for whole rock U–Pb systems applied to the Vredefort crustal profile. J. Geophys. Res. 86, 10681–10687.

Wessel, P., Smith, W.H.F., 1991. Free software helps map and display data. EOS Trans. Amer. Geophys. U. 72 (41), 441.

Zandt, G., Ammon, C.J., 1995. Continental crust composition constrained by measurements of crustal Poisson's ratio. Nature 374, 152–154.

Zandt, G., Myers, S.C., Wallace, T.C., 1995. Crust and mantle structure across the Basin ond Range-Colorado plateau boundary at 37 degrees N latitude and implications for Cenzoic extensional mechanism. J. Geophys. Res. 100, 10529–10548.